DOI: 10.21062/mft.2023.115 http://www.journalmt.com

Research on Elastic Characteristics of Negative Pressure Rubber Isolator

Jianwei Wang (0009-0002-1089-5875)*, Jinlong Feng (0009-0007-9657-9908)
Institute of Mechanical and Electrical Engineering, Lingnan Normal University. Zhanjiang. China. E-mail: wangjw72@163.com
*Corresponding author email: wangjw72@163.com

Aiming at obtaining ultra-low kinematic stiffness and improving the isolation property of low frequency vibration, it is necessary to solve the coupling parameters and rated load of air negative pressure characteristics and rubber characteristics, in order to achieve an ideal elastic characteristic curve of air negative pressure spring. Firstly, the background and working principle of the negative pressure rubber isolation were introduced. In addition, the FEA model of isolator is built based on Mooney-Rivlin constitutive model of rubber. Furthermore, to testify the validity of the mathematical model, the static characteristic and simulation analysis of isolator are studied. The experimental data and characteristic curve of different negative pressure were obtained, the simulated results show a good agreement with those of corresponding experiments. Finally, they also illustrate the validity of the vibration isolation, which realizes better performance of low-frequency vibration isolation.

Keywords: Vibration Isolation, Low-frequency, Constitutive Model, Elastic Characteristics

1 Introduction

It was always a difficult problem to solve the isolation and suppression of low frequency vibrational excitation, because the conventional passive isolation can not satisfy the requirements of low frequency vibration isolation [1-3]. The common rubber vibration isolator has a good vibration isolation result on the vibration frequency within the 5-6Hz range. However, the precision instruments or military products urgently needed vibration frequency below 2Hz [4], it is necessary to develop a new vibration damping device with ultra-low frequency.

It is the focus of many scholars' attention and research how to enhance the existing passive isolation of vibration device to make it have the characteristics of low-frequency or even ultra-low frequency vibration isolation. The vibration isolation effect is better when the stiffness minishes and the natural frequency diminishes. However, the low stiffness will lead to great deformation, and the vibration isolation system is easy to become unstable. Therefore, it is great significant to construct a vibration isolation system with low-frequency vibration isolation effect without affecting the load bearing capacity [5]. Li et al. [6] constructed a composite nonlinear low-frequency vibration isolation system by bonding the inertial structure with the classic ISD vibration isolator. Hu et al. [7] suggested two hybrid-damping models to design quasi-zero stiffness (QZS) isolator prototypes, and proved the isolator can provide a better isolation effect for low-frequency vibration, it is proved that the quasi-zero stiffness vibration isolation is much better than the traditional vibration isolation method by the theoretical derivation and simulation analysis. Tian et al. [8] presented a novel isolator structure which includes three spring HSLD isolators in each corner, the simulation results showed the proposed isolator achieved a remarkable effect on decreasing the peak transmission capacity in the low-frequency band. Wen et al. [9] presented a QZS isolator including viscous damper to enhance the anti-isolation capability of the T-QZS isolators, which can bear a large amplitude of excitation within the scope of vibration-isolation. A called WQZS isolator composed a pair of mutually repulsive magnet rings and a space-saving wave spring was designed, the dynamic model and experimental prototype both are proved its effectiveness [10]. Ye et al. [11] took the butterfly spring as a negative stiffness mechanism to use it in the quasi-zero stiffness vibration isolation structure. An elliptical ring is adopted to carry out a HSLD vibration isolation, and studied the effects of the eccentricity to the vibration isolation effect. [12]. Navazi et al. [13] analysed an unbalanced rotor fixed on HSLDS support and research its vibration and stability. Nonlinear damping can increase the capabilityper of QZS isolators and recognize complex behaviors [14-15].

Although these methods can significantly cut down the system natural frequency, most of them have the disadvantages of complex structure, large occupation area, expensive, and require additional control system, large energy consumption and others. It is difficult to be widely used in practical projects, therefore it is essential to design a new-style low frequency vibration isolator. [19-21]

The remainder of the paper is organized as follows: Section 2 presents the structure and modelling of the suggested isolator. Section 3 introduces the effects of configuration parameters on different negative pressure. Difference matching for stiffness and negative pressure of the isolator is discussed in Section 4. Finally, conclusions are summarized and the future work is explored in Section 5.

2 Materials and Methods

2.1 The principle of negative pressure rubber isolator

The bellows type negative pressure air vibration isolator is mainly composed of cord-rubber composite air bag, upper and lower force panel, inner and outer balance support parts, fixed connection parts, etc. The cord-rubber composite air bag consists of inner and outer sealing tube, cord and vulcanized rubber coating. The sealing layer mainly provides a state of negative pressure or vacuum for the sealed chamber. The inner balance support parts maintain the initial lateral stability to prevent the rubber from shrinking due to the action of negative pressure, it will avoid decreasing the volume of the negative pressure chamber. The cord and vulcanized rubber coating are the main loaded parts. For the sake of the chamber presents a negative pressure state, the external atmosphere pressure will act on the structural shell. The structure schematic drawing of isolator is given as Fig. 1.

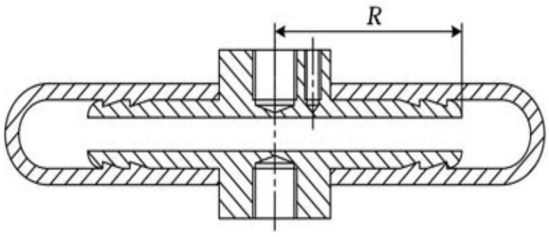

Fig. 1 *The Structure Schematic Drawing of Isolator*

If only considering the stiffness characteristics under negative air pressure, the initial stiffness is large, and gradually decreases and approaches zero with the increase of displacement. However, if only considering the shell of rubber air bag, when the deformation is small, the rubber shell only appears bending deformation, and its stiffness is small, but when the deformation is too large, the rubber shell presents tensile and bending combined deformation, and its stiffness increases rapidly. The two cases do the opposite, both have their advantages and disadvantages. The former cannot be sealed for a long time and has poor impact resistance, while the latter has strong impact resistance and insufficient bearing capacity. Therefore, it is the most significant how to combine the two cases effectively and achieve mutually complementary advantages. It is expected not only to obtain very low stiffness close to the equilibrium position, but also obtain very low natural frequency so as to improve the effectiveness of low-frequency vibration isolation. Meanwhile, when the deformation is too large, the system will not produce too large deflection. It will improve the impact resistance of the system. It is shown as Fig. 2.

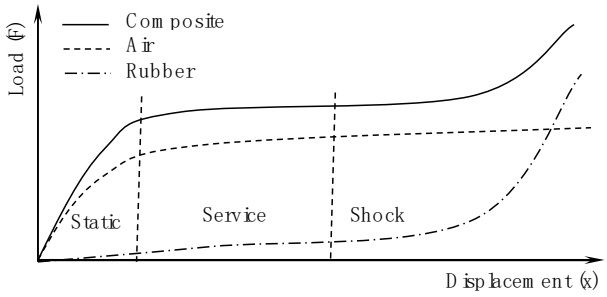

Fig. 2 *Displacement and Load Curve of Different Medium Isolator*

2.2 Mathematical models of negative pressure rubber isolator

The bellow bot of negative pressure rubber isolator is made of rubber composition for coating cords by vulcanizing. For the sake of studying the characteristics of bellow bot, the hyper-elastic constitutive model of rubber was established as follow. Due to the complex molecular properties, geometry and material nonlinear properties of rubber, the stress-strain relationship is complex and the deformation is reversible, it is difficult to describe it by accurate mathematical model. The continuum mechanics is one of the most effective methods. The Mooney-Rivlin model is employed to research the rubber material [9]. The deformation energy of Mooney-Rivlin model can be expressed:

$$U(\varepsilon) = U(I_1, I_2, I_3) \tag{1}$$

$$I_1 = \lambda_1^2 + \lambda_2^2 + \lambda_3^2 \tag{2}$$

$$I_2 = \lambda_1^2 \cdot \lambda_2^2 + \lambda_2^2 \cdot \lambda_3^2 + \lambda_3^2 \cdot \lambda_1^2 \tag{3}$$

$$I_3 = \lambda_1^2 \cdot \lambda_2^2 \cdot \lambda_3^2 \tag{4}$$

$$\lambda_i = 1 + \varepsilon_i \tag{5}$$

Where:

U…Deformation energy [J],

I_1, I_2, I_3…Strain invariants of rubber [-],

λ_i …Principal stretch ratio, i=1,2,3 [-],

ε_i …Strain in three main directions, i=1,2,3 [-].

Take the axis direction as the main direction, because the rubber is the homogeneous and incompressible material. It can be assumed the

uniaxial elongation in tensile direction $\lambda_1 = \lambda$, then the other two directions can be expressed $\lambda_2 = \lambda_3 = \sqrt{\lambda^{-1}}$.

$$\begin{cases} I_1 = \lambda^2 + 2\lambda^{-1} \\ I_2 = \lambda^{-2} + 2\lambda \\ I_3 = 1 \end{cases} \quad (6)$$

It can be deduced by Equation (1)

$$U(\varepsilon) = f(I_1 - 3, I_2 - 3) + g(J - 1) \quad (7)$$

Where:

$f(x)$ …Deviatoric energy function of strain [J],

$g(x)$ …Deviatoric energy function of volumetric strain [J],

J…Coefficient of compressible material [-].

The expression of the deformation energy can be transformed into Equation (8) by deriving Equation (7) using Taylor's expansion.

$$U(\varepsilon) = \sum_{i+j=1}^{N} C_{ij}(I_1 - 3)^i (I_2 - 3)^j + \sum_{i=1}^{N} \frac{1}{D_i}(J - 1)^{2i} \quad (8)$$

Where:

C_{ij} …Expansion coefficient, i,j=0 or 1 [-],

D_i …Model constant [-],

N…Polynomial order [-].

If N=1 in Equation (8), it is the Mooney-Rivlin model. Equation (8) can be expressed Equation (9):

$$U(\varepsilon) = C_{10}(I_1 - 3) + C_{01}(I_2 - 3) + \frac{1}{D_1}(J - 1)^2 \quad (9)$$

Under the Mooney's premise of satisfying the homogeneous and incompressible of rubber, the small deformation of simulated rubber, Equation (9) can be simplified to Equation (10):

$$U(\varepsilon) = C_{10}(I_1 - 3) + C_{01}(I_2 - 3) \quad (10)$$

Where:

C_{10} and C_{01} …Constitutive parameters of the material of Mooney-Rivlin model [-].

They are the positive definite constant [10], then the properties of rubber materials can be simulated well

small and medium strain conditions.

The real stress σ_t and strain ε_t can be calculated by the nominal stress σ_n and nominal strain ε_t:

$$\varepsilon_t = \ln(1 + \varepsilon_n) \quad (11)$$

$$\sigma_t = \sigma_n(1 + \varepsilon_n) \quad (12)$$

The value of C_{10}, C_{01} and D_i can be obtained by experimental data fitting. The parameters in this study are selected as follows: $C_{10} = 3.4MPa$, $C_{01} = 0.78MPa$, $D_1 = 0$.

3 Discussion of results

3.1 Simulation and analysis

The three-dimensional model and finite element model of negative pressure rubber isolator is shown as Figs. 3 and 4. The main specifications of the isolator are given as Table 1.

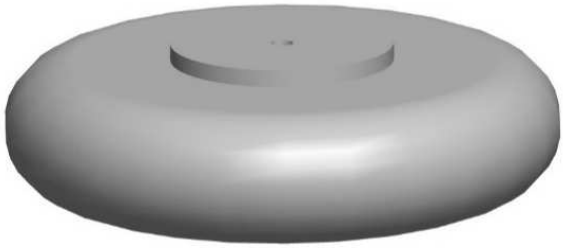

Fig. 3 *Three-dimensional Model of Negative Pressure Rubber Isolator*

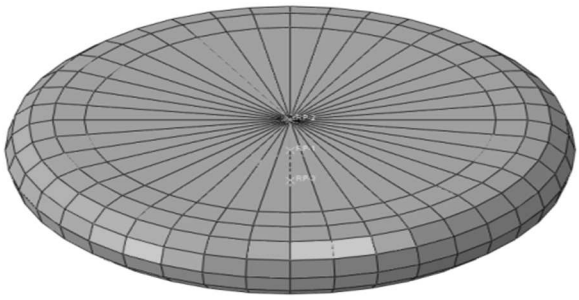

Fig. 4 *Three-dimensional Finite Element Model of Negative Pressure Rubber Isolator*

Tab. 1 *The Main Specifications of Isolator*

Parameters	Value
Young's modulus	210 GPa
Poisson's ratio	0.3
Direction angle	± 45⁰
Design height	55 mm
Maximum diameter	180 mm
Thickness of vulcanizing layer	7 mm
Effective tensile height	40 mm
Maximum working temperature	60 °C

When the stiffness characteristic of the negative pressure air isolator is calculated, the 6 degrees of freedom of upper force panel are constrained to make certain that the negative pressure air isolator is still in the natural state. The rigid contact was used for contact analysis. The 496 units of shell element (S4R) is adopted to calculate the rubber air bag. The 88 units of surface element (SFM3D3) is adopted to calculate the upper and lower force panel. The surface-based fluid cavities are employed to compute the cavity of isolator.

The initial pressure of the cavity is defined by the method of step loading in the finite element model, the initial pressure of the cavity is set 16.33kPa, it is the same as -85kPa negative pressure applied. During the analysis step of loading, the longitudinal degree of freedom of upper force panel is free. The upper force panel is applied 10kN load and the lower force panel remains full restraint. According to the testing method in the national standards GB/T15168-2013, the vacuum treatment is adopted to reduce the cavity pressure of the physical model of negative pressure rubber isolator. The cavity pressure remains about 16.33kPa, then the static experiments have been carried out on WDW-100 electronic universal testing machine and the data of load and displacement are obtained. The experimental system is shown in Fig. 5. The simulation results and the experimental data are indicated in Fig. 6.

Fig. 5 *Experimental system*

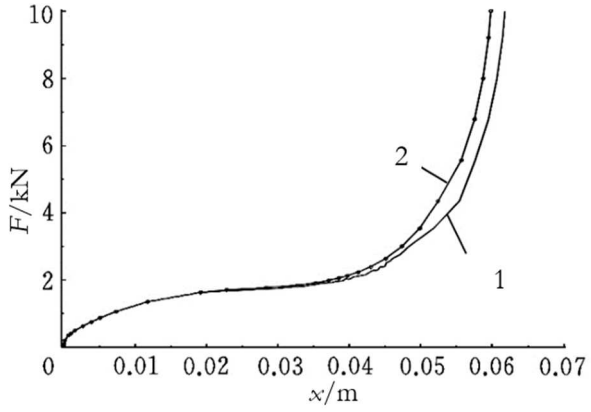

Fig. 6 *Experimental and Simulation Characteristic Curves (1-Experimental data; 2-Simulation data)*

According to the results obtained, the experimental text curve is compared with result of finite element simulation. They are very accordant within 30mm the working stroke. With the increase of travel, the two curves appear deviation, but the trend of the two curves maintains a good consistency, as shown in Fig. 6. It is verified the correctness of finite element model. The stiffness of the characteristic curve is near to zero when the working stroke is 22.5-32.5mm, it indicates that the negative pressure air isolator can obtain quasi-zero stiffness characteristics under this stroke. The operating range of rated load range can be defined within 22.5-32.5mm and the rated working load is close to 2kN. Based on it, a low vibration frequency can be guaranteed. Further analysis reveals that 0-20mm range can be regarded as the static load stage, then the curve stiffness increases rapidly, which indicates the impact resistance is greater. 50-60mm range can be defined the impact resistant working area.

According to the calculation model in Fig. 4, different pressures were applied to the negative pressure cavity respectively, and the load-displacement characteristic curves under different pressure of the negative pressure cavity were obtained, as shown in Fig. 7. The stepped loading method is adopted. Firstly, 30kPa, 45kPa and 60kPa negative pressure are applied to the negative pressure cavity, and then 10kN load is applied respectively. The nonlinearity of the three curves is very large, all of them showed a trend of rising first, then flattening, and finally rising sharply. The principle is consistent with the low-frequency vibration isolation in Fig. 2. The characteristic curve becomes smoother in the working stage with the increasing negative pressure value, and the carrying capacity is greater. Meanwhile, the numerical curves of the negative-pressure cavity pressure with time are shown in Fig. 8 during the tensile testing. The negative-pressure cavity pressure began to drop rapidly and then be steady. Fig. 9 illustrates the numerical curves of the negative-pressure cavity pressure with the tensile displacement. With the increasing of tensile displacement, the negative pressure rises rapidly and presents a high degree of nonlinearity.

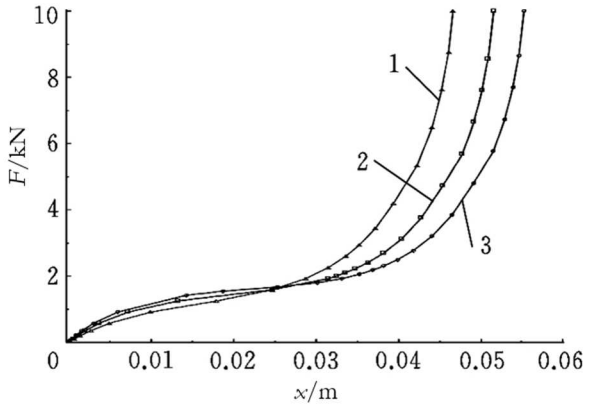

Fig. 7 *Load-displacement curves under different negative pressure (1.p0=30kPa, 2.p0=45kPa, 3.p0=60kPa)*

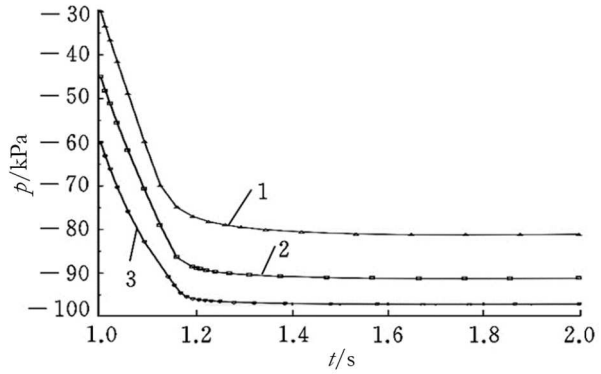

Fig. 8 *Pressure-time curves under different negative pressure (1.p0=30kPa, 2.p0=45kPa, 3.p0=60kPa)*

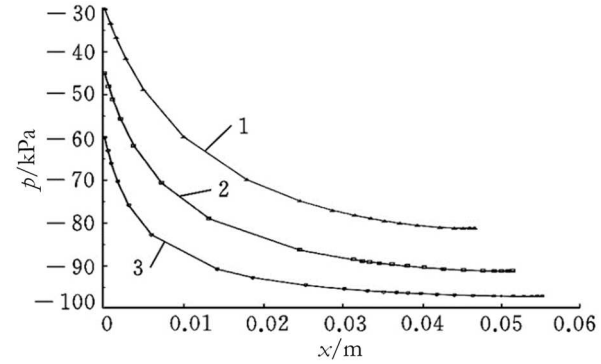

Fig. 9 *Pressure-displacement curves under different initial pressure (1.p_0=30kPa, 2.p_0=45kPa, 3.p_0=60kPa)*

Simulation results show that the load in the static load stage will increase with the increases of negative pressure value, when the working stage is reached, the negative pressure cavity bears the main load. The bending deformation of the rubber bellow in the first two stages begins to transform to tensile deformation. Then the rubber bellow bears the main load.

From what has been mentioned above, the pressure of negative pressure cavity has a direct impact on the stiffness characteristics, which indicates that the higher the negative pressure value, the smaller the stiffness in a reasonable range. The coupling between the negative pressure cavity and the rubber forms a highly nonlinear characteristic curve.

It can be concluded that when only bending deformation occurs, the negative pressure cavity bears the main load, the QZS characteristics can be acquired, and the effectiveness of ultra-low frequency vibration isolation can be achieved.

3.2 Discussion

Based on the above simulation, the presented vibration isolator is seen to be more effective than the existing methods [16-18]. The active control is of advantage in adjusting the equivalent stiffness and damping of the system and can be employed to increase the vibration isolation capability, a means of active isolation [16] which adopted the controllable electromagnetic suspension was studied to widen the isolation frequency range and enhance the isolation capability within the scope of ultra-low frequency. Liu et al. [17] presented a novel elastic origami-inspired structure with characteristics of QZS to achieve obvious low-frequency vibration isolation capability, the effective isolation frequency was below 2 Hz. Han et al. [18] designed a Kresling origami inspired isolator which can effectively control the multiple direction vibration, it revealed full-band frequency vibration isolation for comparatively weak incentives based on its nonlinearity. The simulation results showed that the capability of vibration isolation in the low-frequency range was superior, but the presented structure should be adjusted the parameters m, l, and α to fit for the different applications. However, those systems or structure were usually complex, result in inconvenient adjustment and maintenance. The presented method extended the existing methods, the research results will be very helpful for the improvement of vibration isolation characteristics, and for the design of vibration isolator.

4 Conclusions

The study proposed a new concept of bellow type negative pressure rubber vibration isolator, the following statements could be obtained.

- (1) Basing on the unique features of negative pressure and the better elastic property of rubber, the bellow type negative pressure rubber vibration isolator is presented.
- (2) The system mathematical model is established to analyse the mechanical properties. The theoretical analysis and experimental result reach a good agreement by using the negative pressure vibration isolation theory. The characteristic curves outputted by the experiment further verified the proposed approach is both effective and feasible.
- (3) The proposed vibration isolation method realizes better performance of low frequency vibration isolation. It can set a reference to design and analysis the ultra-low frequency vibration isolation in engineering field.

This project has done some research work in the structural design, simulation analysis, test verification and other aspects of the negative pressure rubber vibration isolator, and has initially achieved relatively ideal scientific research results. However, limited by the existing manufacturing process and experimental

testing equipment, it has not been able to achieve the purpose of quantitative production and even direct application. As future work, two issues must be addressed: 1) how to initially form a set of theories and methods of design the negative pressure rubber vibration isolator; and 2) how to further improve the processing technology and detection of the negative pressure rubber vibration isolator. For the former, one may use the similarity design philosophy to handle the vibration isolation in the engineering field. For the latter, one could attempt to realize product seriation and design standardization to meet different engineering requirements. In addition, the performance of negative pressure rubber vibration isolator in other metrics (i.e., destructive tests and air tightness) will be investigated further.

Acknowledgement

The research is partly supported by the National Natural Science Foundation of China (No. 51275061), The authors acknowledge the Science & Technology Development Special Competitive Project of Zhanjiang City (No. 2020A01010), the Natural Science Research Talents Project of Lingnan Normal University (No. ZL2025).

References

[1] ZHU, S., LOU, J., HE, Q., WENG, X., (2006). *Vibration theory and vibration isolation,* pp.112-125. National Defence Industry Press, Bei Jing. ISBN 7118044687.

[2] QI, W., YAN, G., LU, J., YAN, H., SHI, J., WEI, X., WANG, S., ZHANG, W., (2022). Magnetically modulated sliding structure for low frequency vibration isolation. In: *Journal of Sound and Vibration*, Vol. 526, pp.116819.

[3] WU, J., ZENG, L., HAN, B., ZHOU, Y., LUO, X., LI, X., CHEN, X., JIANG, W., (2022). Analysis and design of a novel arrayed magnetic spring with high negative stiffness for low-frequency vibration isolation. In: *International Journal of Mechanical Sciences*, Vol. 216, pp.106980.

[4] WANG, Q., ZHOU, J., XU, D., OUYANG, H., (2020). Design and experimental investigation of ultra-low frequency vibration isolation during neonatal transport. In: *Mechanical Systems and Signal Processing*, Vol. 139, pp. 106633.

[5] HE, B., YANG, K., WU, S., (2022). Design and Characteristic Analysis of a Tensile Quasi-zero Stiffness Vibration Isolation System. In: *Noise and Vibration Control*, Vol. 42, No. 6, pp. 240-246.

[6] LI, X., SUN, W., SHANG, D., (2022). Analysis of vibration isolation characteristics of a compound nonlinear low frequency vibration isolator. In: *Journal of Ship Mechanics*, Vol. 26, No.7, pp. 1077-1087.

[7] HU, X., ZHOU, C., (2022). The effect of various damping on the isolation performance of quasi-zero-stiffness system. In: *Mechanical Systems and Signal Processing*, Vol. 171, pp.108944.

[8] TIAN, Y., CAO, D., CHEN, C., ZHANG, X., (2023). Vibration isolation performance of a rectangular panel with high-static-low-dynamic stiffness supports. In: *Applied Mathematical Modelling*, Vol. 119, pp. 218-238.

[9] WEN, G., LIN, Y., HE, J., (2022) A quasi-zero-stiffness isolator with a shear-thinning viscous damper. In: *Applied Mathematics and Mechanics*, Vol. 43, No.3, pp. 311-326.

[10] WANG, Q., ZHOU, J., WANG, K., XU, D., WEN, G., (2021). Design and experimental study of a compact quasi-zero-stiffness isolator using wave springs. In: *Science China-Technological Sciences,* Vol. 64, pp. 2255-2271.

[11] YE, K., JI J., FITCH, R., (2023). Further investigation and experimental study of an origami structure-based quasi-zero-stiffness vibration isolator. In: *International Journal of Non-Linear Mechanics*, Vol. 157, pp. 104554.

[12] HAN, W., LU, Z., NIU, M., CHEN, L., (2022). A high-static-low-dynamics stiffness vibration isolator via an elliptical ring. In: *Mechanical Systems and Signal Processing*, Academic, England. Vol. 162, pp. 108061.

[13] NAVAZI, H., HOJJATI, M., (2017). Nonlinear vibrations and stability analysis of a rotor on high-static-low-dynamic-stiffness supports using method of multiple scales. In: *Aerospace Science and Technology*, Vol. 63, pp. 259-265.

[14] GAO, X., TENG, H., (2021). Dynamics and nonlinear effects of a compact near-zero frequency vibration isolator with HSLD stiffness and fluid damping enhancement. In: *International Journal of Non-Linear Mechanics*, Vol. 128, pp.103632.

[15] SLATER, C., OTTO, S., STRANGWOOD, M., (2010). The quasi-static and dynamic testing of damping in golf clubs shafts fabricated from carbon fibre composites. In: *Procedia Engineering*, Vol. 2, No.2, pp.3361-3366.

[16] ZHANG, F., SHAO, S., TIAN, Z., XU, M., XIE, S., (2019).Active-passive hybrid vibration isolation with magnetic negative stiffness

isolator based on Maxwell normal stress. In: *Mechanical Systems and Signal Processing*, Vol. 123, pp. 244-263.

[17] LIU, S., PENG, G., LI, Z., LI, W., SUN, L., (2023). Low-frequency vibration isolation via an elastic origami-inspired structure. In: *International Journal of Mechanical Sciences*, Vol. 260, pp.108622. Elsevier, England. ISSN 0020-7403.

[18] HAN, H., TANG, L., WU, J., SUN, S., YIN, P., CAO D. (2023). Origami-inspired isolators with quasi-zero stiffness for coupled axial-torsional vibration. In: *Aerospace Science and Technology*, Vol. 140, pp. 108438.

[19] TENG TENG, J. T., YAAKOB, M. Y., AMIRHAFIZAN BIN HUSIN, M., MOHAMED, K. A., YUZRINA, M., LAU, W. 2022. Flexural and Out-of-Plane Compression Performance of Hexagonal Rubber Wood Core Sandwich with Increasing Cell Wall Thickness. *Manufacturing Technology*, 22, 240-53.

[20] MÜLLER, M., RUDAWSKA, A., TICHÝ, M., KOLÁŘ, V., HROMASOVÁ, M. 2020. Research on wear resistance of polymeric composite materials based on microparticles from tyre recyclation process. *Manufacturing Technology*, 20, 223-8.

[21] VAŠINA, M., PÖSCHL, M., ZÁDRAPA, P. 2021. Influence of Rubber Composition on Mechanical Properties. *Manufacturing Technology*, 21, 261-9.